NANO LETTERS

2007
Vol. 7, No. 12
3781−3786

Bias-Induced Photoluminescence Quenching of Single Colloidal Quantum Dots Embedded in Organic Semiconductors

Hao Huang,[†] August Dorn,[†] Gautham P. Nair,[†] Vladimir Bulović,*[,‡] and Moungi G. Bawendi*[,†]

Department of Chemistry, Electrical Engineering and Computer Science, Massachusetts Institute of Technology, Cambridge, Massachusetts 02139

Received September 5, 2007; Revised Manuscript Received November 9, 2007

ABSTRACT

We demonstrate reversible quenching of the photoluminescence from single CdSe/ZnS colloidal quantum dots embedded in thin films of the molecular organic semiconductor *N*,*N*′-diphenyl-*N*,*N*′-bis(3-methylphenyl)-(1,1′-biphenyl)-4,4′-diamine (TPD) in a layered device structure. Our analysis, based on current and charge carrier density, points toward field ionization as the dominant photoluminescence quenching mechanism. Blinking traces from individual quantum dots reveal that the photoluminescence amplitude decreases continuously as a function of increasing forward bias even at the single quantum dot level. In addition, we show that quantum dot photoluminescence is quenched by aluminum *tris*(8-hydroxyquinoline) (Alq_3) in chloroform solutions as well as in thin solid films of Alq_3 whereas TPD has little effect. This highlights the importance of chemical compatibility between semiconductor nanocrystals and surrounding organic semiconductors. Our study helps elucidate elementary interactions between quantum dots and organic semiconductors, knowledge needed for designing efficient quantum dot organic optoelectronic devices.

Colloidal semiconductor nanocrystal quantum dots (QDs) have attracted considerable interest in recent years[1−3] due to their spectral tunability, photostability, and chemical versatility. Incorporating colloidal nanocrystals into organic optoelectronic components, such as organic light-emitting devices (OLEDs)[2] and solar cells,[4,5] has been demonstrated and appears promising. At the ensemble level, Ginger and Greenham have studied the interactions between conjugated polymers and CdSe nanocrystals.[6] However, to date little is known about how individual nanocrystals are influenced by the surrounding organic semiconductor matrices. Here, we study interactions between single QDs and two archetypical organic semiconductors: the electron-conducting aluminum *tris*(8-hydroxyquinoline) (Alq_3) and the hole-conducting *N*,*N*′-diphenyl-*N*,*N*′-bis(3-methylphenyl)-(1,1′-biphenyl)-4,4′-diamine (TPD). We investigate the photoluminescence (PL) from QDs in solutions containing Alq_3 or TPD as well as from QDs embedded in evaporated thin films of these materials. Electrodes sandwiching the organic semiconductors allow us to apply an external voltage across the composite organic/QD thin films. Reversible modulation of the QD PL is observed under forward bias. We discuss QD PL quenching mechanisms based on current flow and electric field in the organic/QD films.

The CdSe/ZnS (core/shell) QDs capped with trioctylphosphine oxide were obtained from Quantum Dot Corporation with an emission wavelength centered around $\lambda = 655$ nm. The QDs were first precipitated three times with butanol and methanol and then redispersed in anhydrous chloroform. Alq_3 was purchased from Tokyo Kasei Kogyo Co. Ltd. and purified by resublimation prior to use, while TPD was used as purchased from H.W. Sands Corp.

Quantum dots in solutions containing different concentrations of dissolved Alq_3 or TPD were excited with $\lambda = 525$ nm light generated by a frequency doubled Ti:Sapphire laser. The resulting time-resolved spectra were collected with a streak camera. A band-pass filter ($\lambda = 630$ nm to $\lambda = 680$ nm) was used to suppress emission from the organics and the laser.

The concentration of QDs in chloroform (99%, anhydrous) was ~0.04 μM. Solution A-1 (A-2) was made by adding 1 mg (15 mg) of Alq_3 to 1 mL of QD solution and stirred until the Alq_3 was completely dissolved. Solution A-2 was kept in the dark for ~2 h for this mixing process. Equivalently, two other QD/TPD solutions, T-1 and T-2, were prepared by adding TPD to solvated QDs. A streak camera spectral window of $\lambda = 642$ nm to $\lambda = 668$ nm was

* Corresponding authors. E-mail: (M.G.B.) mgb@mit.edu; (V.B.) bulovic@mit.edu.
[†] Department of Chemistry.
[‡] Electrical Engineering and Computer Science.

10.1021/nl072263y CCC: $37.00
Published on Web 11/23/2007

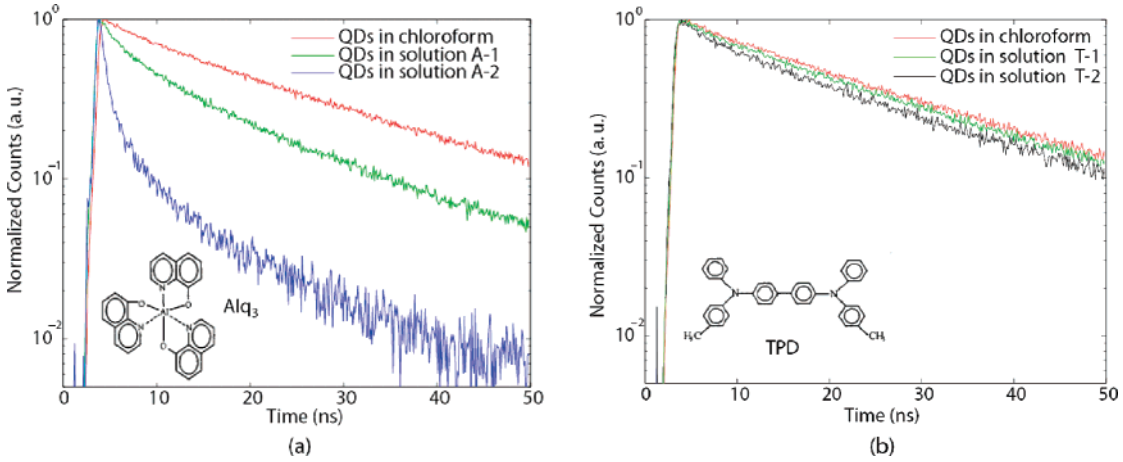

Figure 1. Photoluminescence lifetime measurements of QDs in chloroform solutions containing (a) different concentrations of Alq_3 and (b) different concentrations of TPD. Chemical formulas of Alq_3 and TPD are indicated.

monitored and recorded to determine the luminescence lifetimes of the QDs in different solutions. The PL lifetime of QDs in pure cholorform is ~20 ns. As shown in Figure 1, the QD PL lifetimes of QDs are significantly shortened by Alq_3, while TPD minimally affects QD luminescence. We suspect that 8-hydroxyquinoline functional groups in Alq_3 quench QD PL by interacting with the QD surface. This assumption is consistent with the observation that the PL of QDs in solution is also suppressed when quinoline or 8-hydroxyquinoline is added (data not shown). Förster energy transfer from the QDs to Alq_3 molecules is not probable because of fast exciton relaxation[7] to the band edge of the QDs, which is to the red of the absorption band of Alq_3. TPD on the other hand does not have chelating groups, which explains why no quenching of the PL was observed in solutions T-1 and T-2.

All the measurements above were carried out in dilute QD solutions, while in active optoelectronic devices QDs are embedded in thin solid films.[2,8] To study QD PL in condensed molecular films, we prepared substrates by first RF sputtering 80 nm thick ITO electrode strips through a shadow mask onto 0.13 mm thick cover glass slides. Then a PEDOT solution (BAYTRON CH8000) was spun onto the glass/ITO substrates at 3000 rpm and baked for 30 min. Schematics of the cross-sections of the organic/QD thin film structures with the corresponding electron energy level diagrams are shown in Figure 2. For the device shown in Figure 2a, TPD was added to the QD chloroform solution at a concentration of 10 mg/mL, and the resulting QD/TPD solution was spun onto the device substrates at 3000 rpm in a nitrogen glove box forming a ~50 nm thick film.[8] As described previously, QDs float to the TPD surface due to phase separation.[2] The substrates were then transferred into an evaporator without exposing them to atmosphere, where a 70 nm thick TPD film was deposited at a background pressure of 6×10^{-7} Torr. Then, 100 nm Ag−Mg/20 nm Ag top electrode strips were evaporated through a shadow mask orthogonal to the ITO strips. Rectangular devices with areas of about 2.3 mm^2 each were formed at the intersections of the top and bottom electrodes. For the device shown in Figure 2b, QDs dissolved in chloroform were spun onto a paralene-C coated PDMS stamp at 3000 rpm in a nitrogen glove box. The QDs were then stamped onto a 40 nm thick Alq_3 film that had previously been evaporated onto a PEDOT/ITO/glass substrate.[9] After stamping, a 40 nm thick Alq_3 layer was evaporated onto the QD layer, and Ag−Mg/Ag top electrodes were added as described above. The devices were then packaged in a nitrogen glove box with glass coverslips and UV curable epoxy to minimize device exposure to oxygen and humidity and were mounted onto an *xyz* piezo-stage for measurement.

The $\lambda = 514$ nm line of an Ar-ion laser with an intensity of ~10 W/cm^2 was used as an excitation source. Images were taken through the transparent ITO electrode using a 100× oil immersion objective (Nikon) and an intensified charge-coupled device camera (Pentamax, Princeton Instruments) with a band-pass filter from $\lambda = 630$ nm to $\lambda = 680$ nm. The objective was focused on the fluorescence signal of the QDs under laser excitation, then a voltage was applied to the ITO electrode while the Ag−Mg electrode was grounded. At zero bias, it was easy to observe luminescence from individual QDs in TPD devices, while QD PL was strongly quenched in Alq_3 devices. These observations are consistent with our solution-based measurements (Figure 1). We note that QD PL quenching was less pronounced when QDs were located at an Alq_3-glass or Alq_3-PMMA interface (devices and measurements not shown). This could be due to the presence of dipole layers, surface charges, or a reduced surface coverage of the QDs by Alq_3. We also find that Alq_3 degrades under laser excitation, leading to more QDs becoming visible as Alq_3 degrades. This was also observed for QDs embedded in TPD, however the effect was much less pronounced.

The PL signal from single QDs in Alq_3 is hard to observe even at zero bias, therefore we report only voltage-dependent PL quenching of QDs in TPD. As illustrated in Figure 3a, the decrease in PL intensity coincides with an increase in current flow through the device under forward bias. Under reverse bias, we do not observe any significant current, and PL from the QDs is not quenched. We expect that under reverse bias most of the voltage drops over a thin charge blocking layer at one or both of the organic/electrode

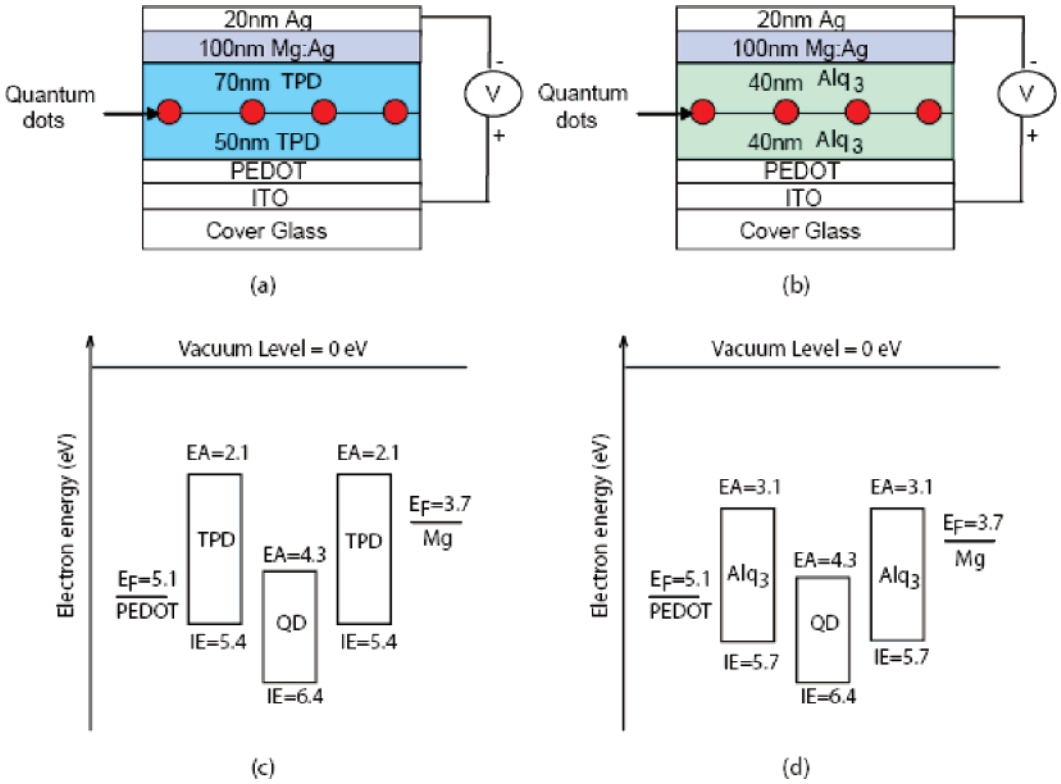

Figure 2. (a,b) Schematic representation of device cross-sections; (c,d) corresponding electron energy level diagrams (not to scale).

interfaces. In this case, the QDs are not exposed to increased electric fields or currents. When a positive voltage is applied to the ITO electrode, the voltage primarily drops across the bulk of the TPD layers, indicating that QDs located approximately at the center of the device are not only subject to an increasing current density, but also to an increasing electric field.[10]

The very dilute QD concentration in our devices enables us to monitor the fluorescence of individual QDs as a function of voltage (Figure 3b). This is of interest because it enables us to observe fluorescence intermittency, or "blinking",[11,12] of individual QDs as well as details of the turning off process that are lost in ensemble averaging. It should be noted that QDs embedded in TPD do not blink as digitally as QDs deposited on clean glass surfaces. The continuous decrease in intensity observed in Figure 3a could be the average of different single QD turning-off behaviors such as: (A) the QDs continue to blink with constant amplitudes but with longer off times or shorter on times or turn off abruptly at different voltages, as illustrated in Figure 4c, and/or (B) the on time amplitude decreases continuously, as illustrated in Figure 4d.

The voltage-dependent PL traces of individual QDs are compared with the ensemble average in Figure 3b. The PL intensity appears to decrease continuously even at the single QD level. To quantify this observation, we plot PL amplitude histograms of the blinking traces of 8 QDs, which were taken over a time period of 40 s with time bins of 0.1 s at a series of constant voltages (Figure 4g). The maximum PL amplitude of every QD at zero bias is normalized to 1. Therefore, at zero bias digital blinking (Figure 4a) leads to two distinct peaks: an "on time amplitude peak" close to 1, and an "off time amplitude peak" close to 0 (Figure 4b). A shrinking on time amplitude peak, which remains fixed at a constant amplitude with increasing bias (schematic in Figure 4e), would indicate longer off times, shorter on times, or abrupt switching off of individual QDs, as proposed in (A). A continuous downward shift in amplitude of the on time amplitude peak (schematic in Figure 4f) on the other hand points toward a continuous decrease in single QD PL intensity, as proposed in (B). As shown in Figure 4g, the on time amplitude peak continuously shifts downward rather than remaining fixed at a constant amplitude and shrinking. This supports the picture proposed in (B).

Because the absorption cross section of QDs is not significantly altered by electric fields,[13] the continuous decrease in PL intensity is the result of a field dependent increase in the ratio of nonradiative to radiative relaxation rates. The field-dependent quenching could be due to the following three mechanisms: (I) Excitons in the QDs are dissociated by the electric field, thus preventing radiative recombination.[14,15] (II) Charge carriers hopping on and off the QDs quench the fluorescence when an excess charge resides in the QD due to an Auger process.[16−18] (III) Excitons in the QDs transfer their energy to the loosely bound charge carriers participating in current flow through the surrounding organic. This mechanism is conceptually similar to the quenching of fluorophores on a metal surface.[19,20]

Jarosz et al.[15] have demonstrated that electric fields in excess of 10^6 V/cm are necessary to completely field ionize excitons in QD films without ligand treatment. However, cap exchanging with shorter ligands can lead to complete exciton ionization at fields as low as 2×10^5 V/cm.[15] In our device, the electrical field strength at the position of the QDs

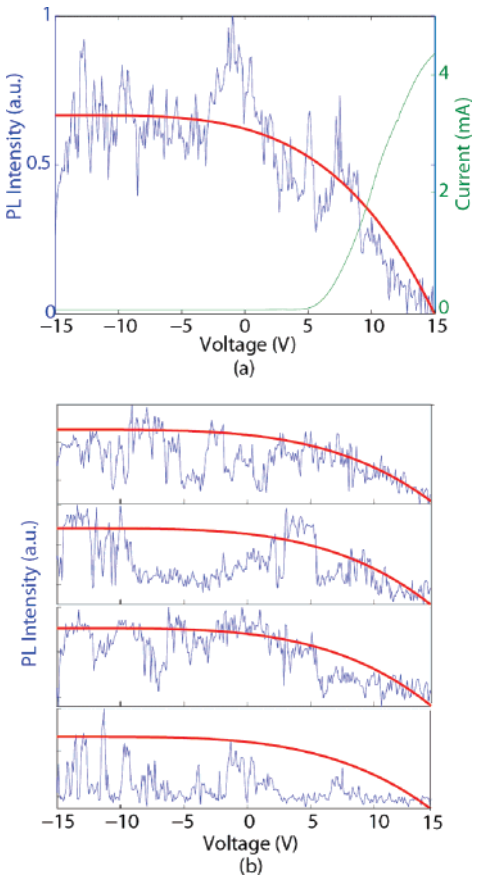

Figure 3. (a) Current−voltage characteristic of the TPD/QD/TPD device of Figure 2a (green curve) and corresponding voltage-dependent PL intensity (blue curve) averaged over 13 QDs. The solid red curve serves as a guide to the eye. (b) PL intensity voltage traces (blue curves) of four individual quantum dots contained in the ensemble. The red curves have the same intensity profile as the red curve in (a).

is linearly approximated as $E = U/d$ under forward bias,[10] where U is the voltage applied across the electrodes and d is the thickness of the organic film. In Figure 3a, we observe near complete QD PL quenching at 15 V corresponding to a field of 10^6 V/cm. Field-induced exciton ionization is more efficient in our devices than in untreated QD films due to the shorter tunneling distance from a QD to a TPD molecule, as compared to the tunneling distance from one QD to the next as considered by Jarosz et al. It is also energetically more favorable for holes to tunnel from a QD to TPD (Figure 2c) than to a neighboring QD. As bias increases, the tunneling rate also increases resulting in PL quenching of the QDs. An increasing exciton ionization rate with increasing bias is also consistent with a continuous decrease in PL amplitude at the single QD level.

To understand the possible contributions from quenching mechanisms II and III, we consider the charge carrier density and the current density at complete quenching around 15 V. TPD thin films are primarily hole conducting with a hole mobility $\mu \sim 10^{-3}$ cm^2/Vs.[21] The hole density ρ is given by

$$\rho = \frac{I}{qS\mu E}$$

where q, S, and I represent unit charge, device area, and current, respectively. At a bias of 15 V, the hole density is on the order of $\sim 10^{15}$ holes/cm^3, which corresponds to one charge carrier in a cube with a side length of ~100 nm. According to the energy band diagram in Figure 2c, the valence band energy level offset between the QDs and TPD impedes hole-injection into the QDs. However, even if hole injection into the QDs were not impeded, for example, due to Fermi level pinning or the presence of surface dipoles, the rate j of holes passing through the cross section of a QD is given by

$$j = \mu E \pi R^2 \rho$$

where R denotes the radius of a QD, which is ~4 nm. The device shows nearly complete QD PL quenching at a bias of 15 V and a current of ~4 mA (Figure 3a), which corresponds to $j = 5 \times 10^5$ hole/s. Within the exciton lifetime of a QD, ~20 ns as measured in solution, there are only $\sim 10^{-2}$ holes passing through the cross-sectional area of a QD. Therefore, charging of the QDs due to current should result at most in quenching on the order of 1%. If holes do not pass through the QDs but remain trapped in the QDs for longer periods of time, this value could be significantly higher. However, the continuous decrease in PL amplitude at the single QD level indicates that the trapping time for charge carriers in a QD must be significantly lower than the binning time of 0.1 s. In addition, it is energetically unfavorable for holes to reside on the QDs, due to the band alignment between the QDs and the surrounding TPD as shown in Figure 2c. Therefore, this scenario appears unlikely. Nearby charge carries can also quench the QDs through energy transfer. In this case, the QD radius has to be replaced by the Förster radius between a charge carrier and a QD. Assuming a Förster radius of ~5 nm,[22] which is close to the radius of a QD, the probability of energy transfer from a QD to a charge carrier is of the same order of magnitude as for charge injection, which is ~1%.

The quenching process is reversible, as demonstrated in Figure 5. The averaged intensity of many individual QDs could be reversibly modulated by ~90% (Figure 5a,c). The turning on and off times are below 5 s and are limited by a convolution of the RC constant of the device, charge rearrangement, and trap filling in the TPD, as well as the time constants of the quenching mechanisms. The continuous decrease in on-time amplitude of individual QDs with increasing electric field as discussed above indicates that the time scale of the quenching mechanism is faster than the binning time of 0.1 s. Therefore, the time constant of the quenching mechanism is not the limiting factor for the turning on and off times.

Given the relatively low carrier density and unfavorable charge injection into QDs, it is therefore likely that electric field-induced exciton ionization is the dominant PL quenching mechanism under forward bias. This interpretation is consistent with results on the electric field-induced quenching of the emission from phosphorescent organic solid-state molecular systems[23] as well as QD films.[15] However, some contributions from quenching mechanisms II and III cannot be ruled out.

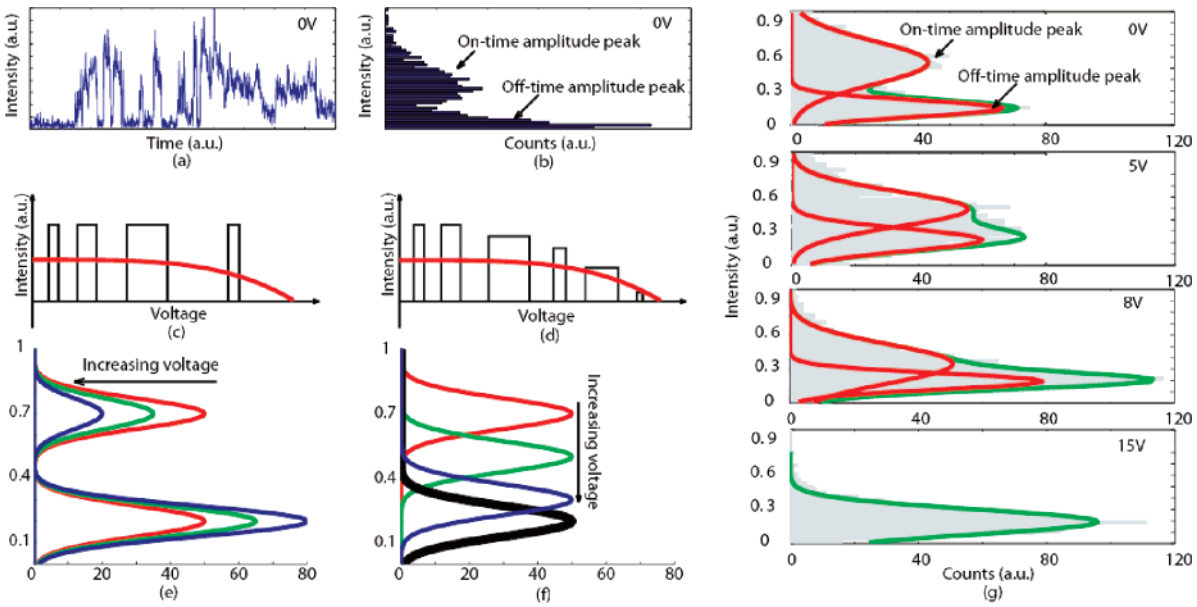

Figure 4. (a) PL intensity trace as a function of time (blinking trace) of an individual QD at 0 V and (b) the corresponding histogram of the PL intensity. (c,d) Schematics illustrating two different turning-off behaviors of individual QDs resulting in the same ensemble averaged PL intensity voltage trace (red curve) and (e,f) corresponding schematics of histograms of the PL intensity at three constant voltages (red, green, and blue). The black curve in (f) is the off-time amplitude peak, which does not vary with voltage. (g) Histograms of the PL intensity distribution of 8 individual QDs at four different constant voltages. At 0, 5, and 8V, the histograms are fitted with two Gaussians (red curves) representing the on-time and off-time amplitude peaks; the green curves are the sum of the two red curves. At 15 V all the QDs are assumed to be off, so the histogram is fitted with one Gaussian only (green curve).

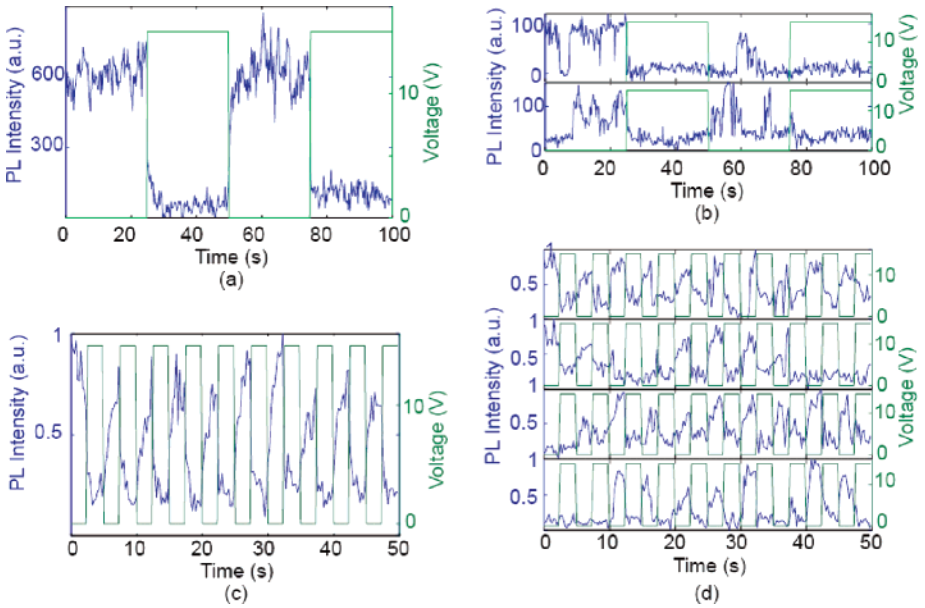

Figure 5. (a,c) Reversible modulation of the PL intensity averaged over 13 individual QDs as a function of voltage. (b,d) Blinking traces of individual QDs under voltage modulation contained in the ensemble averages shown in (a,c), respectively.

We studied the photophysics of quantum dots in solutions and thin film devices containing Alq_3 and TPD. In solution, the fluorescence lifetime of QDs is significantly shortened in the presence of Alq_3, while TPD has little effect. Solutions of quinoline or 8-hydroxyquinoline (the chelating group contained in Alq_3) also quench QD PL. This result highlights the importance of chemical compatibility for devices containing organics and QDs. The solution-based results are consistent with our measurements on QDs embedded in solid-state devices at zero bias. By applying a bias across devices containing QDs embedded in TPD, we can reversibly modulate the photoluminescence intensity of the QDs by 90%. An analysis of several possible quenching mechanisms indicates that field-induced ionization dominates QD PL quenching, which implies that QDs should not be placed in high electric field regions within QD-LED structures. Voltage-dependent PL traces of individual QDs demonstrate that the on-time amplitude of individual QDs decreases continuously as the forward bias increases, consistent with electric field-induced ionization of QD excitons.

Acknowledgment. This research was funded by the HP-MIT Research Alliance, a Presidential Early Career Award for Scientists and Engineers (PECASE), the NSF-MRSEC Program at MIT (DMR-0213282), making use of its shared experimental facilities, the NSF-NSEC Program (DMR-0117795), and an NSF-NIRT (CHE-0507147). A.D. also acknowledges funding from the German National Science Foundation (DFG).

References

(1) Alivisatos, A. P.; Gu, W.; Larabell, C. *Ann. Rev. Biomed. Eng.* **2005**, *7*, 55.
(2) Coe, S.; Woo, W.-K.; Bawendi, M. G.; Bulovic, V. *Nature* **2002**, *420*, 800.
(3) Konstantatos, G.; Howard, I.; Fischer, A.; Hoogland, S.; Clifford, J.; Klem, E.; Levina, L.; Sargent, E. H. *Nature* **2006**, *442*, 7099.
(4) Greenham, N. C.; Peng, X.; Alivisatos, A. P. *Phys. Rev. B* **1996**, *54*, 17628.
(5) Huynh, W. U.; Dittmer, J. J.; Alivisatos, A. P. *Science* **2002**, *295*, 2425.
(6) Ginger, D. S.; Greenham, N. C. *Phys. Rev. B* **1999**, *59*, 10662.
(7) Klimov, V.; McBranch, D. W. *Phys. Rev. Lett.* **1998**, *80*, 4028.
(8) Huang, H.; Dorn, A.; Bulovic, V.; Bawendi, M. G. *Appl. Phys. Lett.* **2007**, *90*, 023110.
(9) Kim, L. Master Thesis, Massachusetts Institute of Technology, Cambridge, MA, 2006.
(10) Schwoerer, M.; Wolf, H. C. *Organische Molekulare Festkorper*; WILEY-VCH: New York, 2005.
(11) Nirmal, M.; Dabbousi, B. O.; Bawendi, M. G.; Macklin, J. J.; Trautman, J. K.; Harris, T. D.; Brus, L. E. *Nature* **1996**, *383*, 802.
(12) Kuno, M.; Fromm, D. P.; Johnson, S. T.; Gallagher, A.; Nesbitt, D. J. *Phys. Rev. B* **2003**, *67*, 125304.
(13) Sacra, A. Doctoral Thesis, Massachusetts Institute of Technology, Cambridge, MA, 1996.
(14) Rothenberg, E.; Kazes, M.; Shaviv, E.; Banin, U. *Nano Lett.* **2005**, *5*, 1581.
(15) Jarosz, M. V.; Porter, V. J.; Fisher, B. R.; Kastner, M. A.; Bawendi, M. G. *Phys. Rev. B* **2004**, *70*, 195327.
(16) Woo, W. K.; Shimizu, K. T.; Jarosz, M. V.; Neuhauser, R. G.; Rubner, M. A.; Bawendi, M. G. *Adv. Mater.* **2002**, *14*, 1068.
(17) Efros, A. L.; Rosen, M. *Phys. Rev. Lett.* **1997**, *78*, 1110.
(18) Shim, M.; Wang, C. J.; Guyot-Sionnest, P. *J. Phys. Chem. B* **2001**, *105*, 2369.
(19) Chance, R. R.; Prock, A.; Silbey, R. J. *Adv. Chem. Phys.* **1978**, *37*, 1.
(20) Barnes, W. L. *J. Mod. Opt.***1998**, *45*, 661.
(21) Stolka, M.; Janus, J. F.; Pai, D. M. *J. Phys. Chem.* **1984**, *63*, 4707.
(22) Kagan, C. R.; Murray, C. B.; Nirmal, M.; Bawendi, M. G. *Phys. Rev. Lett.* **1996**, *76*, 1517.
(23) Kalinowski, J.; Stampor, W.; Mezyk, J.; Cocchi, M.; Virgili, D.; Fattori, V.; Di Marco, P. *Phys. Rev. B* **2002**, *66*, 235321.

NL072263Y